

01

Selecting a fluorescence signal detection mode for DNA melting genetic analysis

© A.L. Bulyanitsa, A.S. Aldekeeva, D.A. Belov

Institute for Analytical Instrumentation of the Russian Academy of Sciences, St. Petersburg, Russia
E-mail: belov.da@list.ru

Received December 1, 2025

Revised January 5, 2026

Accepted January 14, 2026

Successful implementation of the high-resolution melting analysis (HRMA) requires precise provision of temperature conditions. The paper presents the results of numerical modeling of thermal processes in the thermal block of the detecting amplifier, as well as the corresponding analytical solutions in a spatially one-dimensional approximation and with a medium homogeneous in thermal diffusivity. Estimates of the temperature distribution on the detecting amplifier are given when implementing various heating modes in different temperature ranges. The results obtained will reduce the errors in determining the melting temperature, or make the necessary corrections for the systematic error, and can be applied in the development of new devices.

Keywords: DNA melting, temperature field, fluorescence, modeling.

DOI: 10.61011/TPL.2026.05.63285.20587

DNA melting, also known as denaturation or helix–coil transition, is the key source of information about energetics of the DNA double helix [1,2]. Modern high-resolution melting (HRM) analysis is a method for monitoring the dissociation of hydrogen bonds between complementary strands of double-stranded DNA during temperature rise in the presence of fluorescent dyes [3,4]. Differences in the base composition (single nucleotide polymorphism, epigenetic modifications) affect the DNA melting temperature T_m and a shape of the melting curve (fluorescence intensity vs. temperature), which is detected by high-sensitivity instruments — detecting amplifiers [5]. Reliable detection of these differences directly depends on the accurate measurement of T_m [6], and the analysis time depends on the sample temperature variation rate.

High-rate HRM (8 °C/s) has made it possible to improve the analysis reliability, besides the analysis time reduction [7]. In [8], it is shown that minor differences in T_m can be easier detected at higher melting rates. It is important to evaluate the effect of thermal processes caused by the characteristics of instrumental implementation of HRM on the analysis data.

Thermal mode in most of detecting amplifiers is provided by the Peltier elements that have a thermal contact with a metal tube holder, on the one hand, and with a radiator ventilated by air flow from a fan, on the other hand (Figure 1). Tube holder temperature is controlled using the AD590JF (Analog Devices) sensor readings with a maximum absolute error of ± 0.5 °C. Tubes with samples placed in the tube holder wells are hold down on top by a thermal insulation cover, which prevents condensation on tube walls through heating, generally, to 105 °C.

This study proposes a closed-form solution of a thermal diffusivity equation with respect to „averaged“ medium. It is a non-steady-state, spatially one-dimensional equation (normalized vertical z coordinate), where the zero level is a surface (bottom) where temperature is controlled either in a stepwise fashion ΔT or in a linear fashion bt ; constant temperature T_0 is set at the upper boundary. Closed-form solution makes it possible to identify a link between the control temperature at $z = 0$ and temperature boundaries in a tube with a sample and to introduce a bias adjustment for the measurement of T_m .

Transition to one-dimensional simulation is based on solution (infinite sum) for a case [9] with the boundary

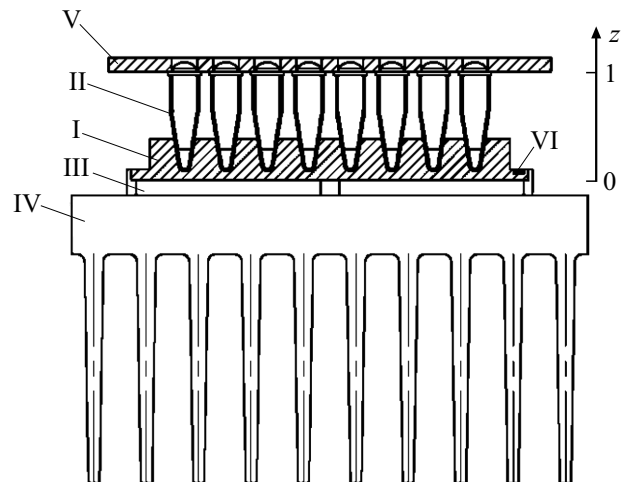


Figure 1. Schematic cross-sectional drawing of the thermal unit of the detecting amplifier. I — tube holder, II — tubes, III — Peltier elements, IV — radiator, V — thermal insulation cover, VI — temperature sensor.

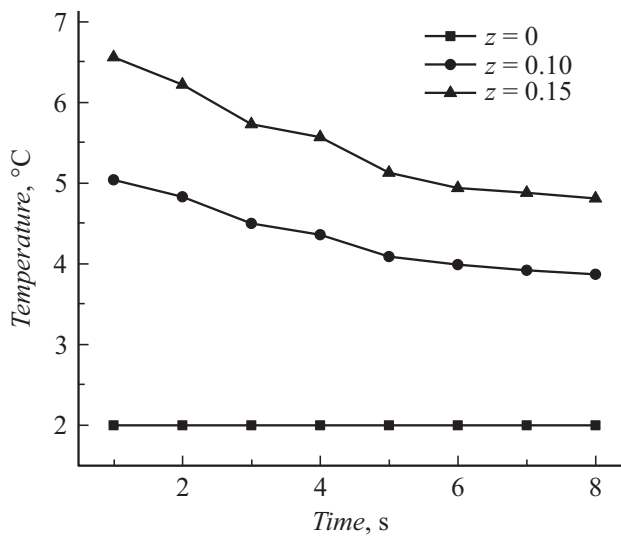


Figure 2. Calculated temperatures at the bottom of the sample ($z = 0.10$) and at the top of the sample ($z = 0.15$); control temperature at the bottom of the tube holder ($z = 0$).

condition $\frac{dT}{dr} + haT = 0$ with low heat exchange ($ha \ll 1$). To evaluate the relation between temperature variations in a radial plane and vertical direction, we can limit ourselves to a summand of a sum with the first positive root of the equation $\gamma_1 J_1(\gamma_1) = ha J_0(\gamma_1)$, where J_k is the Bessel function of the first kind k . Radial temperature variations are defined by variation of the Bessel function from 1 to $J_0(\gamma_1)$, vertical variations are associated with hyperbolic cosine variation from 1 to $ch(\gamma_1 l/a)$. If $ha = 0.3$ is taken as an example, then the Bessel function values range from 0.865 to 1, and for the height/radius ratio $l/a = 5$, the hyperbolic cosine varies within 1–20.748, when using 0.2 ml qPCR tubes (radius 6 mm, height 22 mm) $l/a > 7$. Thus, vertical heat transfer is manifold greater than radial one, and we can limit ourselves to it.

For computational convenience, all temperatures are shifted by the initial temperature level. The least time constant corresponding to the normalized thermal diffusivity coefficient was approximately equal to 2.2 s^{-1} .

The problem of mathematically accurate, but physically approximate tube temperature dependences, which corresponds to $z = [0.1; 0.15]$, is solved by a classical method of separation of variables (Fourier) followed by expansion of solution in eigenfunctions in the form of $\sin(\pi jz)$, $j = 1, 2, \dots$.

For the first case, temperature jump by 2°C at the boundary at the bottom of the tube holder $z = 0$ (set control temperature) and then maintenance of the constant temperature — calculated temperature curves at the bottom of the sample ($z = 0.1$) and at the top of the sample ($z = 0.15$) are shown in Figure 2.

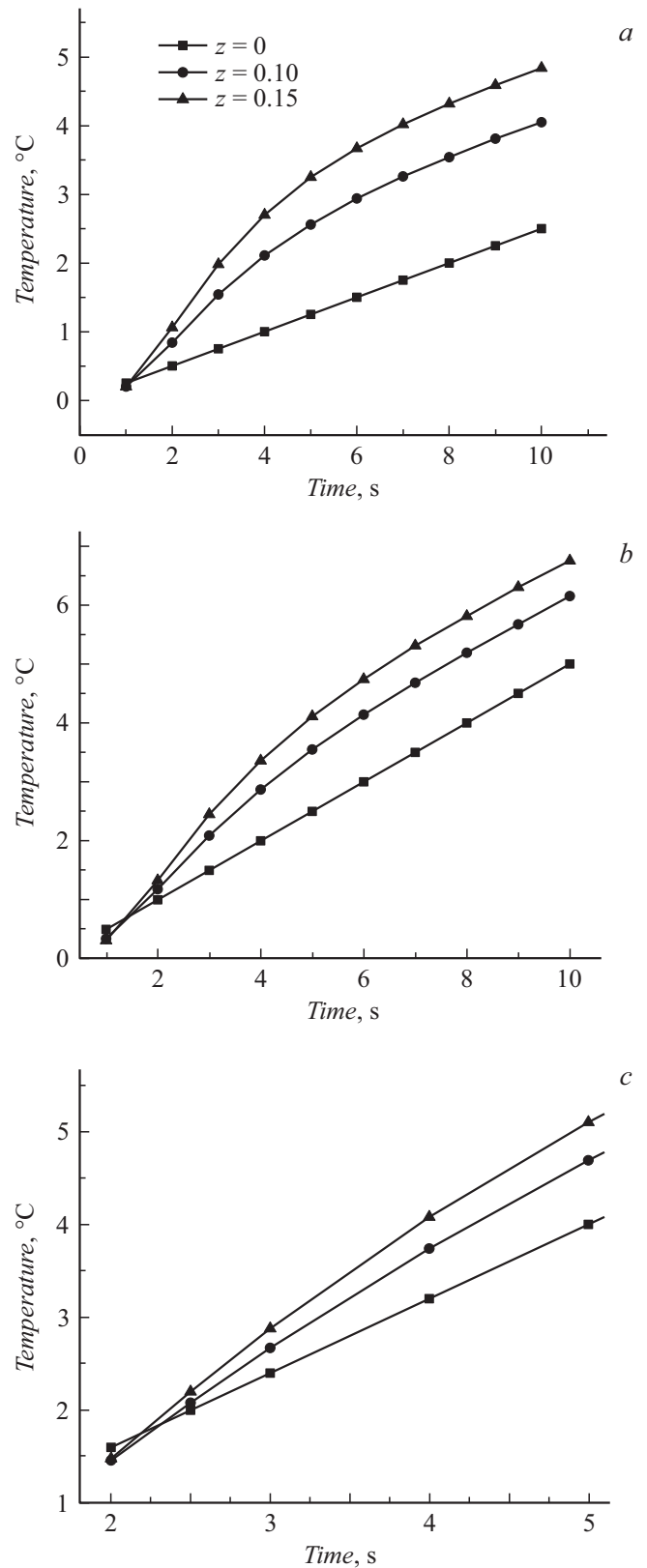


Figure 3. Calculated temperatures in a tube with a sample with linear control bt at $b = 0.25$ (a), 0.5 (b) and 0.8°C/s (c).

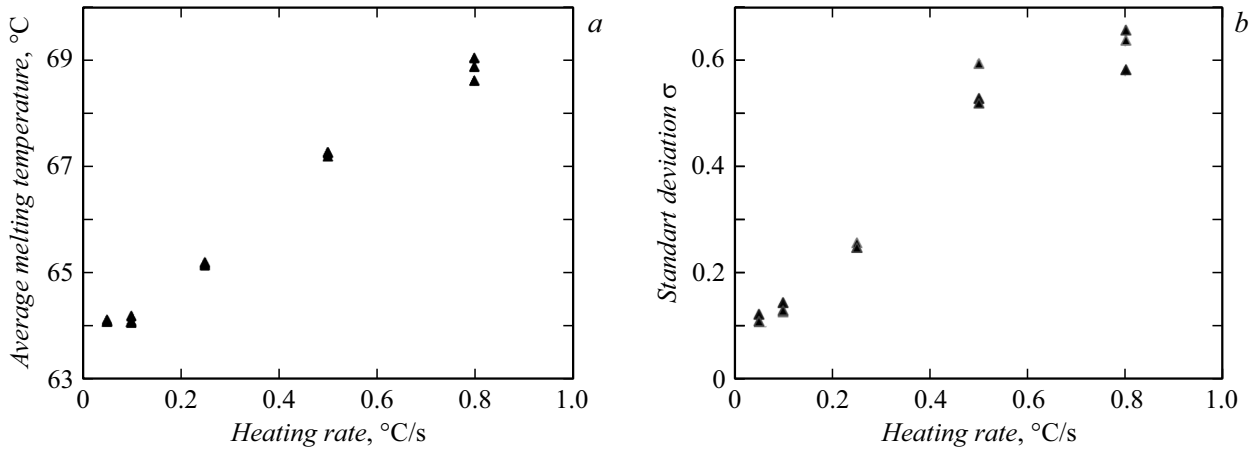


Figure 4. Mean melting temperatures of 48 samples (a) and standard deviation (b) depending on heating rates.

Equations for the method of separation of variables for this thermal diffusivity problem are as follows:

$$T(z, t) = \Delta T + (T_0 - \Delta T)z + \sum_{j=1}^{\infty} \alpha_j \exp(-a^2(\pi j)^2 t) \sin(\pi j z),$$

where

$$\alpha_j = -\frac{2}{\pi j} \left((1 - (-1)^j) \Delta T + (-1)^j (T_0 - \Delta T) \right).$$

There is a systematic substantial divergence between the temperature and control temperature, which declines as the temperature setting process is being completed. Whereas a) significant temperature variations are observed at times exceeding the threefold value of the above-mentioned time constant 2.2 s^{-1} ; b) temperature divergence within a tube decreases from 1.5 C to $\sim 1^\circ \text{C}$.

Figure 3 illustrates the simulated temperature behavior in a tube with a sample for linear control bt with various rates of variation of b . 2°C is reached at 8 s, 4 s and 2.5 s respectively.

Equations for a similar temperature control case are written as

$$T(z, t) = b(1 - z)t + T_0 z + \sum_{j=1}^{\infty} \sin(\pi j z) \left[\beta_j \exp(-a^2(\pi j)^2 t) + \gamma_j (1 - \exp(-a^2(\pi j)^2 t)) \right],$$

where

$$\beta_j = \frac{2T_0(-1)^j}{\pi j},$$

$$\gamma_j = -\frac{2b}{a^2(\pi j)^3}.$$

For the largest of the three heating rate cases, divergence between the tube temperature and control temperature is only $0.08\text{--}0.20^\circ \text{C}$, temperature spread within the sample in the tube is also quite small. The given times are

virtually comparable with the lowest time constant and this temperature distribution state would be far from a steady state, if such state were possible in the present case. Consequently, even within a simulated computational solution, a linear temperature control mode can be defined, that would be the best one in terms of the minimum divergence between the sample temperature and control temperature.

The influence of temperature variation rates on temperature nonuniformity was evaluated via the analysis of T_m of two DNA samples with melting temperatures of about 60°C and 80°C , containing the FAM fluorescent dyes and RTQ1 dyes (Sintol, Russia) covalently attached at the 5'-end and 3'-end, respectively. Melting curves were measured on the ANK-48 amplifier (IAI RAS, Saint Petersburg) with test samples heated in the range of $45\text{--}90^\circ \text{C}$ with preliminary thermostating at 95°C during 60 s.

Curves were processed via sigmoidal function approximation in MATLAB medium with T_m determined by extrema of their first-order derivatives [10].

Data for mean values and standard deviations σ of melting temperatures of two DNA samples in 48 tubes were obtained experimentally in triplicate with five various rates of linear variation of the control temperature bt , where $b = 0.05, 0.1, 0.25, 0.5$ and 0.8°C/s , the total number of measurements was 30 (Figure 4).

When the temperature is set near 60°C , dependence of σ on b has a near-linear form: $\sigma = (0.082 \pm 0.023) + (0.744 \pm 0.053)b$ (coefficient of determination $R^2 \geq 0.93$). The same dependence for the control temperature about 80°C has a similar form: $\sigma = (0.057 \pm 0.031) + (0.716 \pm 0.071)b$ ($R^2 \geq 0.97$). Both dependences don't cross the zero-axis, which can be explained by a random component of temperature measurements, and the factor of increase in σ with a temperature rise can be attributed to the effect of heating nonuniformity enhancement within the tube. For samples with different values of T_m generally varying within

55–95 °C, the identified dependences will maintain their linear mode.

Thus, the assumption [6,7] that it was reasonable to ensure a high sample heating rate to increase the reliability of results obtained by means of the HRM analysis remained unsupported in terms of thermal processes flowing in the thermal unit of the detecting amplifier due to the increase in the temperature field nonuniformity. The identified dependences make it possible to account for the standard component of the measurement error of T_m associated with the difference between the control temperature and the temperature of samples by means of summation with T_m measured by the ANK-48 amplifier.

It is suggested that there are two factors acting in nominally opposite directions and, consequently, there is a nontrivial optimum that allows a fair trade-off to be achieved.

Steady-state temperature distribution within the sample implies linear temperature variation, i.e. temperature difference is set within this sample. For setting the problem of temperature gradient reduction within samples, it is advisable to wait until the steady-state processes are completed and to fix the temperature at times comparable with the lowest time constant.

Funding

This study was funded by the Russian Science Foundation (project No. 24-25-00492).

Conflict of interest

The authors declare no conflict of interest.

References

- [1] A. Vologodskii, M.D. Frank-Kamenetskii, *Phys. Life Rev.*, **25**, 1 (2018). DOI: 10.1016/j.pprev.2017.11.012
- [2] I.V. Likhachev, A.S. Shigaev, V.D. Lakhno, *Phys. Lett. A*, **510**, 129547 (2024). DOI: 10.1016/j.physleta.2024.129547
- [3] C.T. Wittwer, A.C. Hemmert, J.O. Kent, N.A. Rejali, *Mol. Aspects Med.*, **97**, 101268 (2024). DOI: 10.1016/j.mam.2024.101268
- [4] A.A. Fedorov, D.G. Sochivko, D.A. Varlamov, *Tech. Phys.*, **65** (9), 1516 (2020). DOI: 10.1134/S1063784220090169
- [5] I.V. Botezatu, V.N. Kondratova, A.M. Stroganova, *Clin. Chim. Acta*, **551**, 117591 (2023). DOI: 10.1016/j.cca.2023.117591
- [6] O.I. Mir, U.K. Gupta, I. Qasim, A.A. Pandith, F.A. Mir, *Nano TransMed*, **3**, 100047 (2024). DOI: 10.1016/j.ntm.2024.100047
- [7] J.T. Myrick, R.J. Pryor, R.A. Palais, S.J. Ison, L. Sanford, Z.L. Dwight, J.J. Huuskonen, S.O. Sundberg, C.T. Wittwer, *Clin. Chem.*, **65** (2), 263 (2019). DOI: 10.1373/clinchem.2018.296608
- [8] M. Li, R.A. Palais, L. Zhou, C.T. Wittwer, *Anal. Biochem.*, **539**, 90 (2017). DOI: 10.1016/j.ab.2017.10.015
- [9] G.A. Zhukova-Malitskaya, Yu.N. Kuzmin, *Zadachi po matematicheskoi fizike* (LPI, 1984), s. 58. (in Russian)
- [10] V.E. Kurochkin, D.A. Belov, Yu.V. Belov, A.N. Zubik, *Biomed. Eng.*, **55** (5), 333 (2022). DOI: 10.1007/s10527-022-10130-5

Translated by E.Ilyinskaya